AGU PUBLICATIONS

Tectonics

RESEARCH ARTICLE
10.1002/2014TC003698

Key Points:
- Variations in melt production caused by asynchronous rift sector development
- Where the rift narrows, ponding of plume material may enhance melting
- Three-dimensional migration of melt along the LAB focuses magma supply

Correspondence to:
D. Keir,
d.keir@soton.ac.uk

Citation:
Keir, D., I. D. Bastow, G. Corti, F. Mazzarini, and T. O. Rooney (2015), The origin of along-rift variations in faulting and magmatism in the Ethiopian Rift, *Tectonics*, *34*, 464–477, doi:10.1002/2014TC003698.

Received 31 JUL 2014
Accepted 11 FEB 2015
Accepted article online 14 FEB 2015
Published online 18 MAR 2015

The origin of along-rift variations in faulting and magmatism in the Ethiopian Rift

Derek Keir[1], Ian D. Bastow[2], Giacomo Corti[3], Francesco Mazzarini[4], and Tyrone O. Rooney[5]

[1]National Oceanography Centre Southampton, University of Southampton, Southampton, UK, [2]Department of Earth Science and Engineering, Imperial College London, London, UK, [3]Consiglio Nazionale delle Ricerche, Istituto di Geoscienze e Georisorse, Florence, Italy, [4]Istituto Nazionale di Geofisica e Vulcanologia, Pisa, Italy, [5]Department of Geological Sciences, Michigan State University, East Lansing, Michigan, USA

Abstract The geological record at rifts and margins worldwide often reveals considerable along-strike variations in volumes of extruded and intruded igneous rocks. These variations may be the result of asthenospheric heterogeneity, variations in rate, and timing of extension; alternatively, preexisting plate architecture and/or the evolving kinematics of extension during breakup may exert first-order control on magmatism. The Main Ethiopian Rift (MER) in East Africa provides an excellent opportunity to address this dichotomy: it exposes, along strike, several sectors of asynchronous rift development from continental rifting in the south to incipient oceanic spreading in the north. Here we perform studies of volcanic cone density and rift obliquity along strike in the MER. By synthesizing these new data in light of existing geophysical, geochemical, and petrological constraints on magma generation and emplacement, we are able to discriminate between tectonic and mantle geodynamic controls on the geological record of a newly forming magmatic rifted margin. The timing of rift sector development, the three-dimensional focusing of melt, and the ponding of plume material where the rift dramatically narrows each influence igneous intrusion and volcanism along the MER. However, rifting obliquity plays an important role in localizing intrusion into the crust beneath en echelon volcanic segments. Along-strike variations in volumes and types of igneous rocks found at rifted margins thus likely carry information about the development of strain during rifting, as well as the physical state of the convecting mantle at the time of breakup.

1. Introduction

Continental rifts display significant along-strike variations in volumes of magmatism that ultimately causes a heterogeneous igneous record along ancient rifted continental margins. However, there is no consensus on the reasons for spatially variable magmatism during rifting. Increased volumes of magma intrusion have previously been attributed to enhanced melting of the mantle caused by elevated potential temperature [e.g., *White and McKenzie*, 1989; *White et al*., 2008], anomalous volatile content in the asthenosphere [e.g., *Lizarralde et al*., 2007; *Shillington et al*., 2009], or higher extension rate [*Bown and White*, 1995]. Others favor lithospheric hypotheses such as enhanced melting caused by occurrence of some degree of extension and lithospheric thinning prior to arrival of a thermal anomaly [e.g., *Armitage et al*., 2010] or melt migration along the lithosphere-asthenosphere boundary (LAB), with melt focusing greatest where the LAB has steepest gradients [e.g., *Shillington et al*., 2009]. Rifting kinematics has also been suggested to influence the temporal development of melting and locus of intrusion, with oblique extension causing accelerated localization of deformation to a narrow axial zone and facilitating more localized plate thinning [e.g., *Corti et al*., 2003].

The Miocene-Recent Main Ethiopian Rift (MER) accommodates extension between the Nubian and Somalian Plates, constituting the northern part of the East African rift system, and forms the youngest arm of the rift-rift-rift triple junction currently positioned in central Afar (Figure 1) [e.g., *Tesfaye et al*., 2003; *Wolfenden et al*., 2004; *Ayele et al*., 2007]. Plate kinematic models, constrained by GPS data and plate kinematic indicators, indicate extension since at least ~3 Ma has been oriented N95–100°E and occurs at an average rate of ~6 mm/yr (Figure 1) [e.g., *Chu and Gordon*, 1999; *Stamps et al*., 2008; *Kogan et al*., 2012]. Ethiopia offers a unique opportunity to address controls on magma generation and intrusion because from south to north, several stages of rift sector development are exposed, ranging from continental rifting in the south to incipient oceanic spreading in Afar to the north (Figure 1) [e.g., *Hayward and Ebinger*, 1996; *Keir et al*., 2013]. Ongoing seismic and tectonic deformation in the MER [e.g., *Biggs et al*., 2011; *Keir et al*., 2009; *Pagli et al*., 2014] and

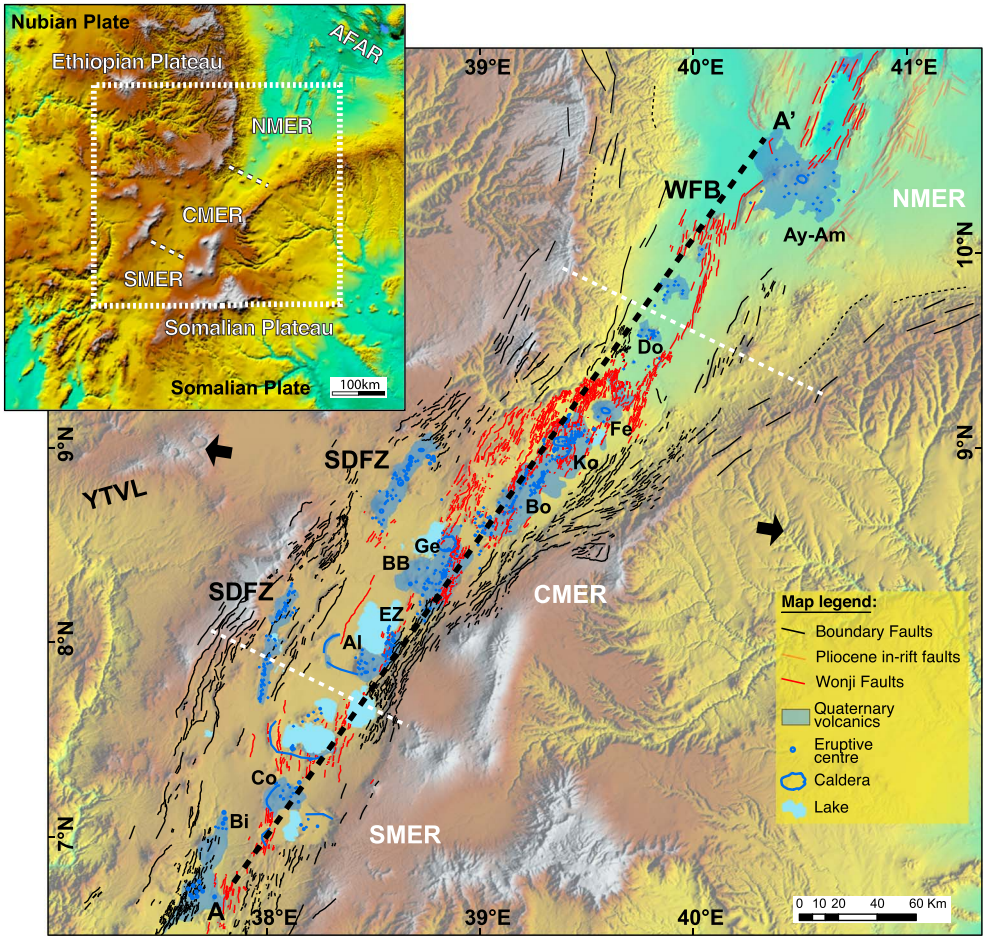

Figure 1. Fault pattern of the Main Ethiopian Rift (MER; modified from *Agostini et al*. [2011a]) superimposed on a digital elevation model (Shuttle Radar Topography Mission data). Inset: the location of the three main rift sectors (Northern, Central, and Southern MER, labeled NMER, CMER, and SMER, respectively). WFB: Wonji Fault Belt, SDFZ: Silti-Debre Zeit Fault Zone. Black arrows show the extension direction [*Kogan et al*., 2012]. The extent of Quaternary-Recent volcanic rocks is taken from *Abebe et al*. [2007]. Letters denote the main volcanic complexes as follows: Al, Aluto; Ay-Am, Ayelu-Amoissa; BB, Bora-Bericha; Bi, Bilate river field; Bo, Boset; Co, Corbetti; Do, Dofen; EZ, East Ziway; Fe, Fentale; Ge, Gedemsa; Ha, Haledebi; and Ko, Kone. White dotted lines show subdivision between SMER, CMER, and NMER.

a plethora of geoscientific constraints from the recent Ethiopia Afar Geoscientific Lithospheric Experiment (see, e.g., *Bastow et al*. [2011] and *Corti* [2009] for reviews) make the region an ideal study locale for continental rifting processes. Crucially, recent work in the MER has provided considerable support for the hypothesis that magmatism plays a fundamental role in achieving extension, without marked crustal thinning, prior to the formation of new ocean basins [*Mackenzie et al*., 2005; *Keir*, 2014].

In this contribution we analyze volcanic vent density to monitor volumes of upper crustal magma intrusion and volcanism along the MER; we also constrain rift obliquity in the Southern Main Ethiopian Rift (SMER), Central Main Ethiopian Rift (CMER), and Northern Main Ethiopian Rift (NMER) sectors in order to explore its influence on magmatic strain localization. A priori constraints on subsurface rift structure and magma intrusion volumes in the MER from controlled-source [e.g., *Keranen et al*., 2004; *Maguire et al*., 2006] and passive-source [e.g., *Daly et al*., 2008; *Kim et al*., 2012] seismic studies, and from gravity surveys [e.g., *Cornwell et al*., 2006], when combined with our new data, provide a clear understanding of lithospheric controls on melt intrusion and volcanism along strike in the MER. Seismological [e.g., *Bastow et al*., 2005, 2008] and petrological/geochemical [e.g., *Rooney et al*., 2012a, 2012b] studies constraining the thermochemical state of the Ethiopian mantle then enable us to study the influence of the convecting asthenosphere on the MER's developing igneous geological record.

2. Tectonics, Volcanism, and Mantle Structure

The MER comprises two distinct systems of normal faults: (1) mid-Miocene border faults and (2) a set of Quaternary-Recent in-rift faults, often referred to as the Wonji Fault Belt (WFB) which mostly developed since ~2 Ma (Figure 1) [*Mohr*, 1967; *Boccaletti et al*., 1998; *Ebinger and Casey*, 2001]. The border faults are typically ~50 km long, have a low density of $<1\ km^{-1}$, and are characterized by large vertical offset (>500 m). Slip on these faults accommodated basin subsidence and gave rise to the prominent escarpments that separate the rift floor from the surrounding plateaus today. In contrast, the younger WFB faults are relatively short (typically <20 km long), closely spaced with a fault density up to $>2\ km^{-1}$, and typically exhibit minor vertical throws of <100 m.

Along the MER, Quaternary-Recent volcanism is dominated by rhyolites, ignimbrites, pyroclastic deposits, and subordinate basalts [*WoldeGabriel et al*., 1990; *Gasparon et al*., 1993; *Boccaletti et al*., 1998; *Trua et al*., 1999; *Peccerillo et al*., 2003; *Rooney et al*., 2012c; *Giordano et al*., 2014]. Magmatic activity is focused along the WFB and the rift marginal Silti-Debre Zeit Fault Zone (SDFZ) and Akaki belts [e.g., *Rooney et al*., 2007, 2014a; *Maccaferri et al*., 2013] (Figure 1). Mafic volcanism along the WFB and SDFZ has taken the form of hundreds of monogenetic basaltic vents consisting of spatter cones, scoria cones, and maars [e.g., *Mazzarini et al*., 2013a]. Analysis of earthquake and vent density shows that the zone of seismicity is generally around 20–30 km wide, while the zone of vents is narrower and centered on the zone of seismicity [*Mazzarini et al*., 2013b]. Intense faulting and a well-developed magma plumbing system (magmas fractionate in the upper ~5 km) characterize the WFB [*Rooney et al*., 2007, 2011]. In contrast, the SDFZ lacks significant surface faulting and is associated with a less well-evolved magmatic system in which magmas fractionate throughout the crust [e.g., *Rooney et al*., 2007, 2011; *Rooney*, 2010; *Mazzarini et al*., 2013a].

The MER comprises three main sectors that have developed asynchronously: the southern, central, and northern MER (Figure 1; the SMER, CMER, and NMER, respectively) [*Abebe et al*., 2010]. The onset of each sector's development is constrained by stratigraphy exposed at the rift margins. In the SMER (Figure 1: south of ~7.5°N), faulting was well established by ~18 Ma [*WoldeGabriel et al*., 1990; *Ebinger et al*., 1993]. In the CMER (Figure 1: 7.5–9.5°N), dating of synrift growth of sedimentary and volcanic sequences, and fission track thermochronology on exposed basement rocks, indicates rapid growth of border faults began between 6 and 11 Ma, somewhat later than in the SMER [*Ukstins et al*., 2002; *Wolfenden et al*., 2004; *Bonini et al*., 2005; *Abebe et al*., 2010]. The western rift shoulder of the CMER is intersected at ~9°N by the Yerer-Tullu Wellel Volcanotectonic Lineament (YTVL), which is thought to be a reactivated Precambrian lineament [e.g., *Abebe et al*., 1998]. The YTVL has experienced volcanism since ~12 Ma [*Abebe et al*., 1998; *Wolfenden et al*., 2004] and lies close to several rift marginal volcanic fields (e.g., SDFZ and Akaki belt) [*Rooney et al*., 2014a]. Low-velocity anomalies in mantle seismic tomographic models at ~75 km depth beneath the YTVL contrast with faster wave speed plateau lithospheric structure to the north and south [e.g., *Bastow et al*., 2005].

North of 9.5°N the NNE trending NMER is set within the Afar depression (Figure 1). Rifting initiated in the southern Red Sea at ~30 Ma [e.g., *Wolfenden et al*., 2005; *Ayalew et al*., 2006] and at ~35 Ma along the full length of the Gulf of Aden (Figure 1) [e.g., *Leroy et al*., 2010]. The NMER therefore bisects lithosphere already extended during ~20 Ma of earlier approximately NE oriented African-Arabian Plate separation [e.g., *Wolfenden et al*., 2004; *Keir et al*., 2011a].

The thermochemical African superplume dominates the mantle structure beneath East Africa in the majority of global tomographic models [e.g., *Li et al*., 2008; *Ritsema et al*., 2011; *Schaeffer and Lebedev*, 2013]. Regional seismic tomographic models also indicate that the MER is underlain by anomalously slow wave speed mantle (see, e.g., *Fishwick and Bastow* [2011] for a review). Mantle wave speeds in Ethiopia are, in fact, amongst the slowest worldwide [*Bastow et al*., 2005, 2008], consistent with the view that the Ethiopian mantle differs markedly from ambient asthenosphere [e.g., *Rooney et al*., 2012a; *Ferguson et al*., 2013]. The low wave speed structure of the Ethiopian mantle is due, at least in part, to elevated mantle potential temperatures of up to ~1490°C [*Rooney et al*., 2012a]. However, the presence of residual melt retained throughout the regional mantle equally plays an important role in the inferred slow seismic wave speeds, which cannot be explained by temperature alone [*Rooney et al*., 2012a].

3. Quantitative Analysis of Rift Kinematics, Vent Density, and Volcanism

In our data analysis, we quantify the relationship between rift kinematics and amount of upper crustal diking and resultant development of aligned cone fields.

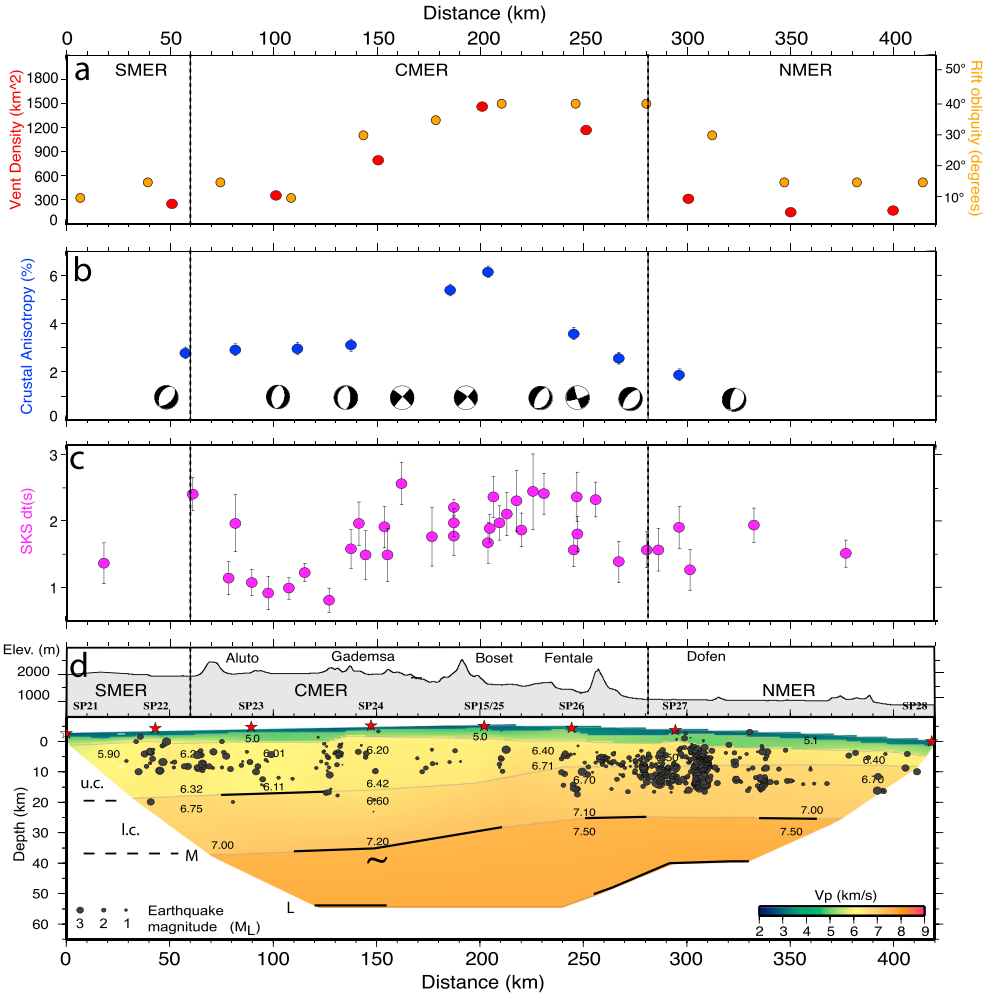

Figure 2. Along-axis variation of geological and geophysical properties in the MER. The position of profile A-A′ is labeled on Figure 1. (a) Orange circles are measurements of rift obliquity, and red circles are measurements of vent density. (b) Crustal seismic anisotropy along the MER [*Keir et al.*, 2011a, 2011b] and a selection of locally representative focal mechanisms. (c) Along-axis variation in SKS splitting delay times with measurements 25 km either side of the middle of the rift axis projected onto the profile [*Kendall et al.*, 2005]. (d) Topographic profile along the rift axis (top) and *P* wave velocity model of *Maguire et al.* [2006] (bottom). Labels are uc: upper crust, l.c: lower crust, M: Mohorovicic discontinuity, and L: mid-Lithosphere reflector. Stars are locations of shot points. Earthquake hypocenters 25 km either side of the center of the rift axis are projected onto the section.

3.1. Rift Kinematics

Rift obliquity (α), the angle between rift extension direction and the direction perpendicular to rift trend, provides a useful measure to describe along-strike variations in MER kinematics. The obliquity angle α has been calculated at 50 km intervals along the MER between 6.5°N and 10.5°N (Figure 2a). For these calculations, the rift trend has been defined as the average orientation of the rift margins, whereas the extension direction has been assumed N100°E trending, based on the available GPS constraints (see above section 1). The SMER extends by approximately pure orthogonal rifting, whereas the CMER extends by low-to-moderate obliquity extension [e.g., *Agostini et al.*, 2011a].

3.2. Vent Density

Monogenetic vents are directly linked to feeder dikes [e.g., *Tibaldi*, 1995; *Connor and Conway*, 2000; *Mazzarini et al.*, 2013b], and their density can be used as an estimation of the degree of diking in the upper crust. To this end, we mapped more than 800 monogenetic vents between 6.5°N and 10.5°N along the MER (Figure 1). Vent separation (nearest neighbor distance) is in the range 0.02–18.7 km, with an average of 0.9 km and

Table 1. Compilation of Obliquity, Vent Density, and Age of the Three Primary Sectors of the Ethiopian Rift

Rift Sector	Latitude (°N)	Obliquity (Deg)	Vent Density (km^2)	Rift Age (Myr)
SMER	<7.5	0–15	290–480	11–20
CMER	7.5–9.5	30–45	800–1500	6–11
NMER	9.5–11	15	130–320	30

standard deviation of 1.6 km. To establish the variations in frequency of near-surface diking, we analyzed the density of volcanic vents using a two-dimensional symmetric Gaussian kernel density estimate [*Connor and Hill*, 1995; *Kiyosugi et al*., 2012]:

$$\lambda(x) = \frac{1}{2\pi N h_i^2} \sum_{i=1}^{N} e^{-\frac{d_i^2}{2h_i^2}} \quad (1)$$

where d_i is the distance between location x and the N vents, and h_i is the smoothing bandwidth for vent i. In this way, the frequency distribution of "neighbor" samples is inferred. Distance values between neighbor samples larger than h_i have a small weight in the computation of the density estimate. We used a variable h value, consisting of the half value of the distance between each sample and its nearest sixth neighbor [*Favalli et al*., 2012]. In addition, we computed the area defined by isodensity (vents/km^2) contours and computed the area that contains more than 90% of sampled vents, assuming these areas are proxy for the diking along the MER. We count the vented areas in 50 km wide windows oriented normal to the NE-SW rift trend. For each scan window the dike intensity is thus expressed as an area (km^2). The wider the vented area, the wider the portion of rift's crust affected by diking. We then project results along a ~400 km long, NE-SW trending along-rift crustal profile (Figure 2a).

4. Results

4.1. Rift Obliquity and Vent Density

The MER shows significant variations in α between the three sectors of the MER (Figure 2). SMER border faults trend ~N10°–25°E, yielding an obliquity of $\alpha = 0$–15°. Axial deformation is not well developed but, where present, is localized to ~N10°–15°E trending normal faults (Figure 1) [*Hayward and Ebinger*, 1996; *Agostini et al*., 2011a; *Corti et al*., 2013]. Diking intensity in the SMER is 290–480 km^2 (Figure 2).

The CMER trends ~N30°–50°E and $\alpha = 30$–45° with respect to the Nubia-Somalia vector. Miocene border faults trend ~N30°–40°E, but Quaternary-Recent WFB axial faults trend ~N15°–20°E [e.g., *Agostini et al*., 2011a]. The oblique extension in the CMER means that the WFB defines a series of right-stepping, en echelon volcanic segments. These are oblique to the rift axis and Miocene border faults but roughly orthogonal to the regional extension direction.

In the CMER, near-surface deformation is concentrated in the WFB and SDFZ, two subparallel belts of focused tectonic-magmatic activity (Figure 1) [e.g., *WoldeGabriel et al*., 1990; *Rooney et al*., 2007, 2011]. Vent density peaks in the CMER at 800–1500 km^2, largely due to increased volcanism along the WFB compared to the SMER and NMER and due to the volcanic chains of the SDFZ near the western rift margin (Figure 2 and Table 1). The increased vent density in the CMER also corresponds to an increase in the surface area of Quaternary-Recent volcanic rocks in this sector of the rift [*Abebe et al*., 2007] (Figure 1).

Quantifying rift obliquity in the NMER is more challenging than in the CMER and SMER, since the Oligocene border faults that define the Afar Depression are mutually perpendicular. We thus instead use the ~N25°–30°E orientation of Late Miocene-to-Pliocene age border faults to define α. The WFB strikes ~N15°–20°E and defines a series of Quaternary-Recent volcanic segments that are mostly colinear except for one major rift-stepping offset at 10°N. Diking intensity in the NMER is 130–320 km^2 (Figure 2 and Table 1). In summary, diking intensity and, by inference, magmatic intrusion within the upper crust are higher by a factor of ~3 in the CMER than in the NMER and SMER. The peak in diking intensity corresponds to a peak in rift obliquity of $\alpha \approx 35$–40° (Figure 2).

4.2. Along-Rift Variations in Seismicity

Along-rift variations in seismicity are well resolved using the dense distribution of seismic stations deployed in the MER during the period 2001–2003 (Figures 2 and 3). In the SMER, earthquakes are distributed across a

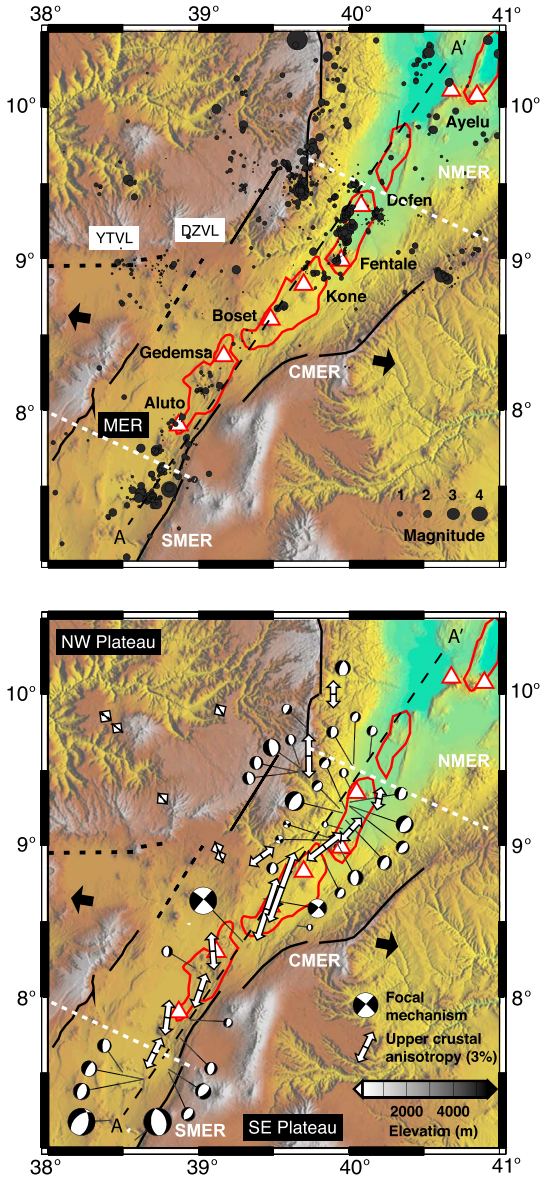

Figure 3. Main geological structures of the Main Ethiopian Rift (MER) plotted on topography. Miocene border faults that bound the rift valley are solid black line. Dashed black lines show prominent off-axis volcanic lineaments: the Debre Zeit Volcanic Lineament (DZVL) and the Yerrer Tulu-Wellel Volcanic Lineament (YTVL). Red lines indicate Quaternary-Recent volcanic segments from *Ebinger and Casey* [2001]; AG: Aluto Gedemsa segment, BK: Boset-Kone segment, and FD: Fentale-Dofen segment. White triangles are major rift volcanoes. The ~N100°E extension direction is shown by black arrows. Profile A-A′ in Figure 2 is marked by dashed line along the axis of the rift. Note that the profile is segmented to capture topography along the central axis of the rift. (top) Seismicity (black dots) recorded during October 2001 to February 2003 with the catalog complete above magnitude 2.1 [*Keir et al.*, 2006]. (bottom) White arrows show percent seismic anisotropy measured from local earthquakes [*Keir et al.*, 2011b]. Arrows parallel to fast polarization direction of the *S* waves; their lengths are scaled according to percent *S* wave anisotropy. Earthquake focal mechanisms are computed from local seismic stations [*Keir et al.*, 2006] and from regional/global data [*Foster and Jackson*, 1998; *Ayele*, 2000].

50 km wide zone that includes the eastern rift flank border fault. This pattern of strain is consistent with the broad zone of collapse calderas and faults observed at the surface [e.g., *Le Turdu et al.*, 1999; *Agostini et al.*, 2011b; *Corti et al.*, 2013]. Seismicity in the CMER and NMER is generally characterized by earthquakes on the normal fault networks of the WFB, with the volcanic centers themselves being relatively aseismic. In the Fentale-Dofen volcanic segment at 9–9.5°N, for example, seismicity along the rift axis is concentrated at 9–14 km depth within a narrower (30 km wide) axial graben that is coincident with the 20–30 km wide zone of mafic intrusion [*Keir et al.*, 2009]. Most earthquakes are normal dip slip on NNE striking, axial parallel faults. Vertical *P* axes and *T* axes parallel to the extension direction (Figures 2 and 3) are consistent with the style of faulting. In the Boset-Kone volcanic segment at 9–9.5°N, low seismicity and the absence of earthquakes deeper than ~10 km (Figures 2 and 3) are indicative of elevated heat flow suppressing brittle deformation [e.g., *Beutel et al.*, 2010; *Daniels et al.*, 2014]. Focal mechanisms in the CMER include strike-slip earthquakes with rift-parallel *P* axes and *T* axes that parallel rift opening (Figures 2 and 3). This is controlled by the obliquity of the CMER, with normal faulting within volcanic segments and strike-slip faulting in the transfer zones connecting them.

4.3. Geophysical Indicators of Along-Rift Variations in Melt Emplacement and Production

Wide-angle seismic experiments reveal a ~35–40 km thick crust in the SMER (Figure 2), which is ~10 km thinner than beneath the adjacent plateaus [*Mackenzie et al.*, 2005; *Maguire et al.*, 2006; *Keranen et al.*, 2009]. The crust thins to ~28 km between 8 and 9.5°N in the CMER, but there is little evidence for further crustal thinning in the NMER (Figure 2) [*Maguire et al.*, 2006]. *P* wave speeds (V_p) in the lower crust range from 6.6 to 7.2 km/s, peaking at 7.1–7.2 km/s in the lowermost crust between Gedemsa and Fentale volcanoes in the CMER (Figure 2). Elevated wave speeds of >6.8 km/s have been interpreted as evidence for gabbroic crustal intrusions [e.g., *Keranen et al.*, 2004; *Mackenzie et al.*, 2005]. In the upper crust, 3-D controlled-source tomography

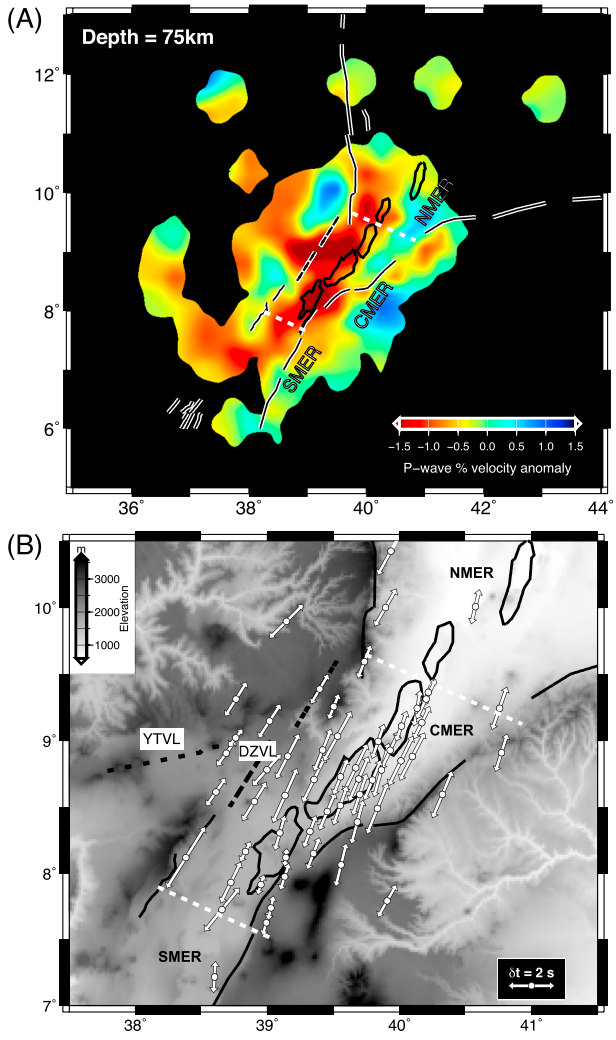

Figure 4. (a) *P* wave velocity structure beneath the Ethiopian Rift (MER), adjacent plateaus, and southern Afar at 75 km depth from the study of *Bastow et al.* [2008]. Mid-Miocene border faults of the MER and pre-Miocene border faults of the Red Sea and Aden Rifts (black and white lines) define the primary topographic expression of the rift. Volcanically active Quaternary-Recent rift segments define the axis of the central northern MER. (b) Direction and magnitude of *S* wave anisotropy measured using SKS splitting [*Kendall et al*., 2005]. Arrow direction is parallel to fast polarization direction, and arrow length is scaled to amount of splitting. Border faults and segments are as in Figure 4a.

shows significant variation in V_p, with discrete high V_p (>6.4 km/s) zones beneath the volcanic segments. Anomaly amplitudes peak beneath the Boset-Kone segment in the CMER [*Keranen et al*., 2004].

Broadband seismological studies constrain the distribution and orientation of melt production, percolation, and intrusion into the mantle lithosphere and into the crust. Studies of mantle seismic anisotropy demonstrate that across the MER, fast polarization directions (ϕ) mirror the ~30° difference in strike between MER border faults and axial volcanic segments [*Kendall et al*., 2005] (Figure 4). This was interpreted as melt intrusion localized through the lithosphere since the Quaternary [*Kendall et al*., 2005]. However, the magnitude of anisotropy is highest beneath the border faults, an observation interpreted as enhanced melt extraction and flow along the steeply dipping lithosphere-asthenosphere boundary (LAB) [*Kendall et al*., 2005]. Evidence for an extension-related control on mantle seismic anisotropy beneath the MER also comes from back azimuthal variations in S_V and S_H, derived from dispersion analysis of Rayleigh and Love waves, respectively. These data point strongly toward an oriented melt pocket mechanism of seismic anisotropy, with the implication that elongate melt intrusions characterize the MER lithosphere between 20 and 75 km depth [*Kendall et al*., 2006; *Bastow et al*., 2010].

Within the MER, SKS splitting delay times (δt) increase northward from $\delta t = 1$–1.5 s in the SMER to ~2.5 s in the CMER (Figures 2 and 4). In the NMER, δt falls to ~1.5 s, remaining relatively constant into central Afar and Djibouti [*Ayele et al*., 2004; *Kendall et al*., 2006; *Gao et al*., 2011; *Hammond et al*., 2014]. Seismic anisotropy peaks in the CMER, consistent with the view that MER melt volumes are highest there. Studies of crustal seismic anisotropy tell a similar story, with shear wave splitting delay times from ~6 to 10 km deep local earthquakes higher at $\delta t = 0.24$ s (6% anisotropy) in the CMER than in the SMER and NMER where $\delta t = 0.1$–0.15 s, ~3% anisotropy [*Keir et al*., 2011b] (Figures 2 and 4).

The correlation shown between the peak in SKS delay times and intensity of upper crustal intrusions provides strong evidence that variations in melt generation in the mantle and transport in the deep lithosphere are broadly responsible for along-rift variations in intrusion and volcanism. Such an inference is consistent with regional-scale relative arrival time mantle tomographic inversions [e.g., *Bastow et al*., 2005, 2008] that demonstrate that the lowest wave speeds in the uppermost mantle beneath the MER are lowest beneath the CMER (Figure 4). However, the lowest wave speeds do not lie directly beneath the present-day locus of strain, the WFB, and are instead offset toward the rift flanks and mirroring the half-graben rift morphology that

characterized the early mechanical stages of MER development in Miocene times (Figure 4). As mentioned earlier, preexisting base of lithosphere topography is also thought to play a role in governing melt migration beneath the region [e.g., *Bastow et al*., 2005, 2008].

The lowest uppermost mantle wave speeds beneath the CMER lie beneath the intersection of the YTVL and CMER, not beneath the rift axial Quaternary magmatic segments. Segmentation of the mantle low wave speed anomalies is also on longer length scale (~150 km) than the ~60 km long crustal segments above them [*Bastow et al*., 2005, 2008]. These observations suggest that a first-order connection between crust and mantle magmatic processes in the MER does not exist, in contrast to the ocean basins where mantle anomalies reflect segmentation along the spreading ridges [e.g., *Wang et al*., 2009]. Processes such as lateral melt migration are thus required to transport melt generated in the mantle toward the rift axis [*Bastow et al*., 2005].

5. Discussion

Global variations in the amount of magma intrusion and volcanism during the transition between continental rifting and initial seafloor spreading are commonly attributed to increased melt production caused by elevated asthenospheric potential temperature [*White et al*., 2008], mantle composition [*Lizarralde et al*., 2007], active upwelling [*Holbrook et al*., 2001], and increased extension rate or shorter duration of rifting [*Bown and White*, 1995]. We have established, using analysis of variations in volcanic cone distribution, clear evidence for along-rift variations in volcanism and crustal magma intrusion that correlate spatially with geophysical indicators of increased melt intrusion in the deeper lithosphere and enhanced melt production in the asthenosphere. However, there exists a wide array of processes that may impact these observations. In the discussion below we explore these processes and examine whether mantle geodynamic and/or plate tectonic processes provide clearest answers for the observed variations in melt production and intrusion in the MER.

5.1. Controls on Along-Rift Variations in Magma Generation

Observations of variations in the volume of magma intrusion into the continental lithosphere could, to first order, be explained by heterogeneity in the generation of magmas along a continental rift. Fundamentally, the variable supply of such magma could reflect in the degree of magma intrusion into the continental lithosphere—much in the same manner as at an oceanic spreading center. Below we examine the potential mechanisms that could promote variable along-rift magma production in the MER.

5.1.1. The Afar Plume and Mantle Potential Temperature

Quaternary-Recent basalts erupted in the Gulf of Aden, Afar, and the MER preserve details of the mantle reservoirs that currently contribute to melt generation in the region. Studies of these magmas have revealed that their geochemical characteristics may be described in terms of mixing between the ambient depleted upper mantle, the African lithosphere, and the Afar plume [*Hart et al*., 1989; *Schilling et al*., 1992; *Deniel et al*., 1994; *Furman et al*., 2006; *Rooney et al*., 2012b]. Elevated mantle potential temperatures associated with the Afar plume could result in variable degrees of magma generation within the region as mixing between the plume, depleted mantle, and lithospheric reservoirs is variable both in a spatial [*Schilling et al*., 1992; *Rooney et al*., 2012b] and temporal sense [*Rooney et al*., 2013] and could result in along-rift changes in magma production.

The isotopic characteristics of primitive basalts erupted in the WFB and SDFZ in the central and northern MER show the clear influence of the "C" mantle reservoir, interpreted as representing contribution of the Afar plume to magma generation [e.g., *Furman et al*., 2006; *Rooney et al*., 2012b]. Anomalously hot and buoyant plume material may flow along channels of thin lithosphere [e.g., *Sleep*, 2008], such as beneath the MER, and regions of preexisting lithospheric thinning like the YTVL. Previous studies have raised the possibility of such processes controlling magmatism throughout the African continent [*Ebinger and Sleep*, 1998]. In particular, there is clear evidence that the flow of channelized plume material is a first-order control on magmatism in the Gulf of Aden [*Schilling et al*., 1992; *Leroy et al*., 2010] and MER [*Rooney et al*., 2012b, 2013]. The influence of this plume component on magmatism broadly decreases southward along the rift [*Rooney et al*., 2012b]. However, the distribution of recent rift magmatism does not correlate with a simple model of a southward decrease in the Afar plume component.

Evidence of the interaction between channelized plume flow and lithospheric structure along the Gulf of Aden and MER [e.g., *Rooney et al*., 2007; *Leroy et al*., 2010] suggests that while the plume material influences melt generation, the precise mechanisms of melt generation are more complex. Previous studies have

highlighted the role of segmentation and discontinuities in the Gulf of Aden spreading axis leading to disruption of axial flow and the formation of off-axis magmatism [*Leroy et al*., 2010]. In the MER, southward thickening of the lithosphere occurs in the CMER where magmatism is particularly focused [*Bonini et al*., 2005; *Rooney et al*., 2007] (Figure 2). The geochemistry of the volcanic rocks in this region is consistent with the southward increase in LAB depth acting as an obstruction to the southward flow of plume material, with potential application to understanding the spatial pattern of magma generation and intrusion.

5.1.2. Volatile Enrichment of the Mantle

Heterogeneity in melt production can be facilitated by selective hydration of the mantle. However, the sublithospheric reservoirs contributing the magma generation in Afar (i.e., the depleted mantle and Afar plume) are not notably enriched in volatiles. Specifically, the East African depleted mantle is not impacted by modern subduction, and mantle plumes such as the Afar plume are not notably hydrated [e.g., *Dixon et al*., 2002]. Hydrous phases do, however, exist within the Ethiopian subcontinental lithospheric mantle [*Ferrando et al*., 2008; *Frezzotti et al*., 2010]. Melt generation through thermobaric perturbation of such phases may result in melt production [*Rooney et al*., 2014b], but the absence of the unusual isotopic and trace element values that typify ancient hydrated domains in Quaternary rift basalts argues against such hydration as a primary control on magma generation along the rift.

5.1.3. Along-Rift Variations in Extension Rate

Geodynamic models indicate that increased extension rate causes increased melt production [*Bown and White*, 1995], with the implication that along-strike changes in extension rate could cause along-rift variations in melting. However, in the sectors of the MER we analyze, both current and past plate motions predicted from plate kinematic models show no significant variations in extension rate nor amount of extension, for at least the last ~3 Ma [e.g., *Chu and Gordon*, 1999; *Stamps et al*., 2008]. Neither variation in amount or rate of extension explains variations in magmatism.

5.1.4. Asynchronous Rift Sector Development

The MER is the youngest rift of the Afar triple junction with plate reconstructions constrained with geochronology and structural data suggesting that the NMER within the Afar depression overprints lithosphere stretched by ~19 Ma pre-MER extension forming the Red Sea and Gulf of Aden [e.g., *Tesfaye et al*., 2003; *Wolfenden et al*., 2004] (Figure 1). This stepped along-rift variability in duration of lithospheric stretching where the MER emerges into Afar explains spatially coincident stepped thinning of the crust and mantle lithosphere [*Maguire et al*., 2006] (Figure 2). Extension is also thought to have been initiated earlier at ~10–20 Ma in the SMER than in the central MER at ~6–11 Ma [*WoldeGabriel et al*., 1990; *Ebinger et al*., 1993; *Bonini et al*., 2005]. Therefore, available constraints suggest that the CMER has a younger history of rifting than elsewhere in the MER, with the implication that the thermal anomaly created by upwelling asthenosphere in this sector of the rift has not yet cooled to that of the surrounding material [*Bastow et al*., 2005, 2008] (Figure 4). A younger history of plate stretching may therefore contribute to increase magma production in the CMER. The younger age of the CMER would also mean that there has been less time for magmas to be extracted from the mantle, which would also explain the lower mantle velocities there.

5.2. Mechanisms That Facilitate Heterogeneity in Magma Intrusion Into the Continental Lithosphere

We have noted that asynchronous rift sector development and the obstruction to southward flow of plume material at the CMER are potential controls on causing heterogeneities in along-rift melt production. Next we examine the impact that rift architecture and kinematics has on melt emplacement in the lithosphere and its resulting impact on the degree and distribution of intrusion and volcanism.

5.2.1. Melt Focusing by Steep Gradients on the LAB

The spatial coincidence of along-axis lithospheric thinning in the CMER with the peaks in crustal and mantle anisotropy (Figures 2), and the zone of lowest wave speeds beneath the MER [*Bastow et al*., 2008] (Figure 4), suggests a causative link. The elevated SKS splitting delay times at the flanks of the MER supports a mechanism of enhanced melt production and melt migration along steep gradients on the LAB beneath the margins of the MER [*Kendall et al*., 2005; *Holtzman and Kendall*, 2010]. The along-rift peak in SKS splitting in the CMER, coincident with along-rift thinning of the lithosphere, suggests that three-dimensional (3-D) variations in LAB topography may also be important in focusing melt supply (Figure 5). In addition, in the CMER, the orientation of the low seismic velocity anomaly at 75 km is beneath and parallel to the YTVL. However, the SKS splitting fast directions are orthogonal to that and rift parallel, supporting the assertion of melt intrusion once in the lithosphere is controlled by the regional tectonic stresses [*Rooney et al*., 2014a].

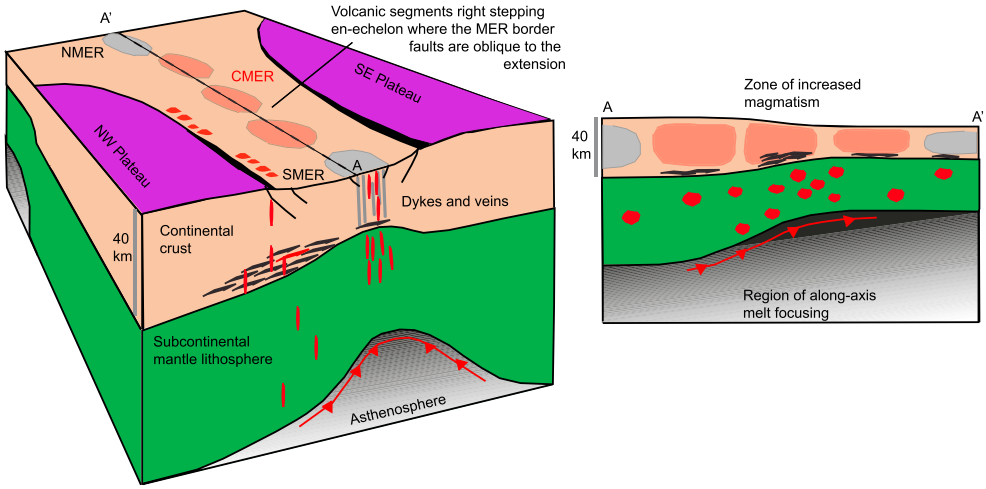

Figure 5. Conceptual model for the creation of enhanced magma production and supply beneath the MER. (left) Cross-rift section illustrating enhanced melting along the lithosphere-asthenosphere boundary (LAB) beneath the margins of the MER. Melt is predominantly focused at shallower depths to the rift axis following strain gradients and intruding the crust as dense mafic sills and dikes. Some melt is also supplied to rift margin magmatic systems. (right) Along-rift section displaying enhanced melt production from the presence of along-axis thinning of the MER as the rift valley opens into the Afar depression stretched by prior extension of the southern Red Sea and western Aden Rifts.

Three-dimensional focusing of melt is an important process at mid-ocean ridges, where melts are generated over a relatively broad region in the mantle, but magmatic addition to the crust occurs primarily at the ridge axis due to melt migration along the base of the lithosphere [e.g., *Magde and Sparks*, 1997]. Such a mechanism not only accounts for across-rift variation in magmatism but can also explain enhanced magmatism beneath segment centers where the lithosphere is locally thinned [e.g., *Dunn et al.*, 2005]. Locally enhanced magma production along steep gradients of the LAB also explains the abrupt transition from magma-rich to magma-poor rifting during continental breakup in the eastern Black Sea [*Shillington et al.*, 2009]. In this setting, migration of melts occurs subvertically from the base of the melting zone to the LAB, with the addition of lateral vector caused by melt migration along the steeply inclined LAB. Migration of melt along the LAB focuses crustal magmatic accretion to a relatively short, narrow zone in the rift axis that eventually evolves into volcanic segments in an incipient seafloor spreading system. Such a mechanism of along- and across-rift thinning of the lithosphere in the CMER likely plays an important role in melt migration and emplacement (Figure 5).

5.2.2. Localized Extension due to Oblique Rifting

While the peak in magmatism in the CMER can be broadly explained by variable melt supply caused by asynchronous rift sector development, 3-D melt focusing, and ponding of plume material, the specific location and length scales of mantle anomalies show anticorrelation with the crustal zones of magmatism in the WFB [*Bastow et al.*, 2005, 2008]. Instead, an increase in crustal intrusions and volcanism appears to peak coincidently with variations in rift obliquity and lie directly beneath the surface expression of the Quaternary-Recent volcanic segments (Figures 1 and 2).

Both numerical [*van Wijk*, 2005] and analogue models [*Corti*, 2008; *Agostini et al.*, 2009] of lithospheric thinning for rifts at varying obliquity demonstrate that after an initial phase of boundary fault activity localized thinning of the lithosphere occurs in axial pockets oriented roughly perpendicular to extension. For the same amount of bulk extension and similar amounts of lithospheric thinning, the degree of strain localization from border faults to rift axis increases with increasing obliquity [e.g., *Agostini et al.*, 2009]. In the CMER, higher rift obliquity favors early abandonment of boundary faults and early shift to localized faulting in the WFB within the rift floor. This in turn should correspond to a more localized thinning of the plate with the implication that decompression melting could be more focused beneath rifts undergoing low-to-moderate obliquity extension than beneath orthogonal rifts. Numerical models of low-obliquity volcanic ocean ridges support this hypothesis, where the segmented and localized upwelling and mantle melting help explain increased volcanism at some ridges such as the Mohns and Reykjanes ridges [*van Wijk and Blackman*, 2007].

In addition, recent numerical models of continental breakup [*Brune et al*., 2012; *Heine and Brune*, 2014] suggest that oblique extension facilitates rifting and breakup at lower forces than for orthogonal extension, with a fundamental implication that oblique rifting occurs more rapidly [*Ebinger and van Wijk*, 2013] with resultant increased melting from faster plate thinning [*Bown and White*, 1995]. Additionally, rapid and localized faulting and fracturing of the crust induced by oblique extension are likely to aid transport and intrusion of melt into the upper crust and eventual eruption at the WFB.

6. Conclusions

Along-strike variations in geological geophysical properties of the MER provide a unique 3-D snapshot of deformation and magma production beneath a developing magmatic rift. Ethiopia's widespread, voluminous magmatism is the result of continental breakup above a thermochemically anomalous mantle. Along-strike variations in magma intrusion and volcanism are broadly explained by variations in melt production caused by asynchronous rift sector development. Additionally, where the rift dramatically narrows, ponding of southward flowing plume material from Afar may enhance melting, and 3-D migration of melt along steep gradients of the LAB likely focuses magma supply into the plate. Our analysis also indicates that rifting obliquity likely aids localizing crustal intrusion beneath en echelon volcanic segments during rifting. Along-rift variations in magmatism are unlikely due to variations in mantle potential temperature, water content, and extension rate. Therefore, along-strike variations in volumes and types of igneous rocks found at rifted margins may thus carry considerable information concerning history and architecture of the rift, as well as the thermochemical state of the convecting mantle at the time of breakup.

Acknowledgments
Derek Keir acknowledges funding provided by a CNR short-mobility grant and from NERC grant NE/L013932/1. Ian Bastow acknowledges support from the Leverhulme Trust. The data for this paper are available from the IRIS Data Management System. Seismic equipment from SEIS-UK is funded by NERC under agreement R8/H10/64. We also thank the Associate Editor of tectonics and two anonymous reviewers for their constructive feedback.

References

Abebe, B., V. Acocella, T. Korme, and D. Ayalew (2007), Quaternary faulting and volcanism in the Main Ethiopian Rift, *J. Afr. Earth Sci.*, *48*, 115–124.
Abebe, T., F. Mazzarini, F. Innocenti, and P. Manetti (1998), The Yerer-Tullu Wellel volcanotectonic lineament: A transtensional structure in central Ethiopia and the associated magmatic activity, *J. Afr. Earth Sci.*, *26*, 135–150.
Abebe, T., M. L. Balestriri, and G. Bigaazi (2010), The Central Main Ethiopian Rift is younger than 8 Ma: Confirmation through apatite fission-track thermochronology, *Terra Nova*, *22*, 470–476, doi:10.1111/j.1365-3121.2010.00968.x.
Agostini, A., G. Corti, A. Zeoli, and G. Mulugeta (2009), Evolution, pattern, and partitioning of deformation during oblique continental rifting: Inferences from lithospheric-scale centrifuge models, *Geochem. Geophys. Geosyst.*, *10*, Q11015, doi:10.1029/2009GC002676.
Agostini, A., M. Bonini, G. Corti, F. Sani, and F. Mazzarini (2011a), Fault architecture in the Main Ethiopian Rift and comparison with experimental models: Implications for rift evolution and Nubia-Somalia kinematics, *Earth Planet. Sci. Lett.*, *301*, 479–492, doi:10.1016/j.epsl.2010.11.024.
Agostini, A., M. Bonini, G. Corti, F. Sani, and P. Manetti (2011b), Distribution of Quaternary deformation in the central Main Ethiopian Rift, East Africa, *Tectonics*, *30*, TC4010, doi:10.1029/2010TC002833.
Armitage, J. J., J. S. Collier, and T. A. Minshull (2010), The importance of rift history for volcanic margin formation, *Nature*, *465*, 913–917, doi:10.1038/nature09063.
Ayalew, D., C. Ebinger, E. Bourdon, E. Wolfenden, G. Yirgu, and N. Grassineau (2006), Temporal compositional variation of syn-rift rhyolites along western margin of the southern Red Sea and northern Main Ethiopian Rift, *Geol. Soc. London Spec. Publ.*, *259*, 121–130.
Ayele, A. (2000), Normal left-oblique fault mechanisms as an indication of sinistral deformation between the Nubia and Somalia Plates in the Main Ethiopian Rift, *J. Afr. Earth Sci.*, *31*(2), 359–368.
Ayele, A., G. Stuart, and J.-M. Kendall (2004), Insights into rifting from shear wave splitting and receiver functions: An example from Ethiopia, *Geophys. J. Int.*, *157*, 354–362.
Ayele, A., G. Stuart, I. Bastow, and D. Keir (2007), The August 2002 earthquake sequence in north Afar: Insights into the neotectonics of the Danakil microplate, *J. Afr. Earth Sci.*, *40*, 70–79.
Bastow, I. D., G. W. Stuart, J.-M. Kendall, and C. J. Ebinger (2005), Upper-mantle seismic structure in a region of incipient continental breakup: Northern Ethiopian Rift, *Geophys. J. Int.*, *162*, 479–493, doi:10.1111/j.1365-246X.2005.02666.x.
Bastow, I. D., A. A. Nyblade, G. W. Stuart, T. O. Rooney, and M. H. Benoit (2008), Upper mantle seismic structure beneath the Ethiopian hot spot: Rifting at the edge of the African low-velocity anomaly, *Geochem. Geophys. Geosyst.*, *9*, Q12022, doi:10.1029/2008GC002107.
Bastow, I. D., S. Pilidou, J.-M. Kendall, and G. Stuart (2010), Melt-induced seismic anisotropy and magma assisted rifting in Ethiopia: Evidence from surface waves, *Geochem. Geophys. Geosyst.*, *11*, Q0AB05, doi:10.1029/2010GC003036.
Bastow, I. D., D. Keir, and E. Daly (2011), The Ethiopia Afar Geoscientific Lithospheric Experiment (EAGLE): Probing the transition from continental rifting to incipient seafloor spreading, *Geol. Soc. Am. Spec. Pap.*, *478*, 51–76, doi:10.1130/2011.2478(04).
Beutel, E., J. van Wijk, C. Ebinger, D. Keir, and A. Agostini (2010), Formation and stability of magmatic segments in the Main Ethiopian and Afar Rifts, *Earth Planet. Sci. Lett.*, *293*, 225–235, doi:10.1016/j.epsl.2010.02.006.
Biggs, J., I. D. Bastow, D. Keir, and E. Lewi (2011), Pulses of deformation reveal frequently recurring shallow magmatic activity beneath the Main Ethiopian Rift, *Geochem. Geophys. Geosyst.*, *12*, Q0AB10, doi:10.1029/2011GC003662.
Boccaletti, M., M. Bonini, R. Mazzuoli, B. Abebe, L. Piccardi, and L. Tortorici (1998), Quaternary oblique extensional tectonics in the Ethiopian Rift (Horn of Africa), *Tectonophysics*, *287*, 97–116.
Bonini, M., G. Corti, F. Innocenti, P. Manetti, F. Mazzarini, T. Abebe, and Z. Pècksay (2005), The evolution of the Main Ethiopian Rift in the frame of Afar and Kenya rifts propagation, *Tectonics*, *24*, TC1007, doi:10.1029/2004TC001680.
Bown, J. W., and R. S. White (1995), Effect of finite extension rate on melt generation at rifted continental margins, *J. Geophys. Res.*, *100*, 18,011–18,029, doi:10.1029/94JB01478.
Brune, S., A. A. Popov, and S. V. Sobolev (2012), Modeling suggests that oblique extension facilitates rifting and continental break-up, *J. Geophys. Res.*, *117*, B08402, doi:10.1029/2011JB008860.

Chu, D., and R. G. Gordon (1999), Evidence for motion between Nubia and Somalia along the Southwest Indian Ridge, *Nature*, *398*, 64–67.
Connor, C. B., and F. M. Conway (2000), Basaltic volcanic fields, in *Encyclopedia of Volcanoes*, edited by H. Sigurdsson, pp. 331–343, Academic Press, New York.
Connor, C. B., and B. E. Hill (1995), Three non-homogeneous Poisson models for the probability of basaltic volcanism: Application to the Yucca Mountains region, Nevada, *J. Geophys. Res.*, *100*, 10,107–10,125, doi:10.1029/95JB01055.
Cornwell, D. G., G. D. Mackenzie, R. W. England, P. K. H. Maguire, L. M. Asfaw, and B. Oluma (2006), Northern Main Ethiopian Rift crustal structure from new high-precision gravity data, *Geol. Soc. London Spec. Publ.*, *259*, 307–321.
Corti, G. (2008), Control of rift obliquity on the evolution and segmentation of the Main Ethiopian Rift, *Nat. Geosci.*, *1*, 258–262, doi:10.1038/ngeo160.
Corti, G. (2009), Continental rift evolution: From initiation to incipient break-up in the Main Ethiopian Rift, East Africa, *Earth Sci. Rev.*, *96*, 1–53, doi:10.1016/j.earscirev.2009.06.005.
Corti, G., M. Bonini, S. Conticelli, F. Innocenti, P. Manetti, and D. Sokoutis (2003), Analogue modelling of continental extension: A review focused on the relations between the patterns of deformation and the presence of magma, *Earth Sci. Rev.*, *63*, 169–247, doi:10.1016/S0012-8252(03)00035-7.
Corti, G., M. Philippon, F. Sani, D. Keir, and T. Kidane (2013), Re-orientation of the extension direction and pure extensional faulting at oblique rift margins: Comparison between the Main Ethiopian Rift and laboratory experiments, *Terra Nova*, doi:10.1111/ter.12049.
Daly, E., D. Keir, C. J. Ebinger, G. W. Stuart, I. D. Bastow, and A. Ayele (2008), Crustal tomographic imaging of a transitional continental rift: The Ethiopian Rift, *Geophys. J. Int.*, *172*, 1033–1048, doi:10.1111/j.1365-246X.2007.03682.x.
Daniels, K. A., I. D. Bastow, D. Keir, R. S. J. Sparks, and T. Menand (2014), Thermal models of dyke intrusion during development of continent-ocean transition, *Earth Planet. Sci. Lett.*, *385*, 145–153, doi:10.1016/j.epsl.2013.09.018.
Deniel, C., P. Vidal, C. Coulon, and P. J. Vellutini (1994), Temporal evolution of mantle sources during continental rifting: The volcanism of Djibouti (Afar), *J. Geophys. Res.*, *99*, 2853–2869, doi:10.1029/93JB02576.
Dixon, J. E., L. Leist, C. Langmuir, and J. G. Schilling (2002), Recycled dehydrated lithosphere observed in plume-influenced mid-ocean-ridge basalt, *Nature*, *420*, 385–389.
Dunn, R. A., V. Lekic, R. S. Detrich, and D. R. Toomey (2005), Three-dimensional seismic structure of the Mid-Atlantic Ridge (35°N): Evidence for focused melt supply and lower crustal dike injection, *J. Geophys. Res.*, *110*, B09101, doi:10.1029/2004JB003473.
Ebinger, C., and J. W. van Wijk (2013), Roadmap to continental rupture: Is obliquity the route to success, *Geology*, *42*, 271–272.
Ebinger, C. J., and M. Casey (2001), Continental breakup in magmatic provinces: An Ethiopian example, *Geology*, *29*, 527–530.
Ebinger, C. J., and N. H. Sleep (1998), Cenozoic magmatism throughout East Africa resulting from impact of a single plume, *Nature*, *395*, 788–791.
Ebinger, C. J., T. Yemane, G. Woldegabriel, J. L. Aronson, and R. C. Walter (1993), Late Eocene-Recent volcanism and faulting in the southern Main Ethiopian Rift, *J. Geol. Soc.*, *150*, 99–108, doi:10.1144/gsjgs.150.1.0099.
Favalli, M., S. Tarquini, P. Papale, A. Fornaciai, and E. Boschi (2012), Lava flow hazard and risk at Mt. Cameroon volcano, *Bull. Volcanol.*, *74*, 423–439, doi:10.1007/s00445-011-0540-6.
Ferguson, D. J., J. Maclennan, I. D. Bastow, D. M. Pyle, S. M. Jones, D. Keir, J. D. Blundy, T. Plank, and G. Yirgu (2013), Melting during late-stage rifting in Afar is hot and deep, *Nature*, *499*, 70–73, doi:10.1038/nature12292.
Ferrando, S., M. L. Frezzotti, E. R. Neumann, G. De Astis, A. Peccerillo, A. Dereje, Y. Gezahegn, and A. Teklewold (2008), Composition and thermal structure of the lithosphere beneath the Ethiopian plateau: Evidence from mantle xenoliths in basanites, Injibara, Lake Tana Province, *Mineral. Petrol.*, *93*, 47–78.
Fishwick, S., and I. D. Bastow (2011), Towards and better understanding of African topography: A review of passive-source seismic studies of the African crust and upper mantle, *Geol. Soc. London Spec. Publ.*, *357*, 343–371.
Foster, A. N., and J. A. Jackson (1998), Source parameters of large African earthquakes: Implications for crustal rheology and regional kinematics, *Geophys. J. Int.*, *134*, 422–448.
Frezzotti, M. L., S. Ferrando, A. Peccerillo, M. Petrelli, F. Tecce, and A. Perucchi (2010), Chlorine-rich metasomatic H2O–CO2 fluids in amphibole-bearing peridotites from Injibara (Lake Tana region, Ethiopian plateau): Nature and evolution of volatiles in the mantle of a region of continental flood basalts, *Geochim. Cosmochim. Acta*, *74*, 3023–3039.
Furman, T., J. Bryce, T. Rooney, B. Hanan, G. Yirgu, and D. Ayalew (2006), Heads and tails: 30 million years of the Afar plume, *Geol. Soc. London Spec. Publ.*, *259*, 95–119.
Gao, S. S., K. H. Liu, and M. G. Abdelsalam (2011), Seismic anisotropy beneath the Afar Depression and adjacent areas: Implications for mantle flow, *J. Geophys. Res.*, *115*, B12330, doi:10.1029/2009JB007141.
Gasparon, M., F. Innocenti, P. Manetti, A. Peccerillo, and A. Tsegaye (1993), Genesis of the Pliocene to Recent bimodal mafic-felsic volcanism in the Debre Zeyt area, central Ethiopia: Volcanological and geochemical constraints, *J. Afr. Earth Sci.*, *17*, 145–165.
Giordano, F., M. D'Antonio, L. Civetta, S. Tonarini, G. Orsi, D. Ayalew, G. Yirgu, D. Dell'Erba, M. A. Di Vito, and R. Isaia (2014), Genesis and evolution of mafic and felsic magmas at Quaternary volcanoes within the Main Ethiopian Rift: Insights from Gedemsa and Fanta'Ale complexes, *Lithos*, doi:10.1016/j.lithos.2013.08.008.
Hammond, J. O. S., J.-M. Kendall, J. Wookey, G. W. Stuart, D. Keir, and A. Ayele (2014), Differentiating flow, melt, or fossil seismic anisotropy beneath Ethiopia, *Geochem. Geophys. Geosyst.*, *15*, 1878–1894, doi:10.1002/2013GC005185.
Hart, W. K., G. Woldegabriel, R. C. Walter, and S. A. Mertzman (1989), Basaltic volcanism in Ethiopia: Constraints on continental rifting and mantle interactions, *J. Geophys. Res.*, *94*, 7731–7748, doi:10.1029/JB094iB06p07731.
Hayward, N. J., and C. J. Ebinger (1996), Variations in the along-axis segmentation of the Afar Rift system, *Tectonics*, *15*, 244–257, doi:10.1029/95TC02292.
Heine, C., and S. Brune (2014), Oblique rifting of the Equatorial Atlantic: Why there is no Saharan Atlantic Ocean, *Geology*, *42*, 211–214, doi:10.1130/G35082.1.
Holbrook, W. S., et al. (2001), Mantle thermal structure and active upwelling during continental breakup in the North Atlantic, *Earth Planet. Sci. Lett.*, *190*, 251–266, doi:10.1016/S0012-821X(01)00392-2.
Holtzman, B. K., and J.-M. Kendall (2010), Organized melt, seismic anisotropy and plate boundary lubrication, *Geochem. Geophys. Geosyst.*, *11*, Q0AB06, doi:10.1029/2010GC003296.
Keir, D. (2014), Magmatism and deformation during continental breakup, *Astron. Geophys.*, *55*, 5.18–5.22.
Keir, D., C. J. Ebinger, G. W. Stuart, E. Daly, and A. Ayele (2006), Strain accommodation by magmatism and faulting as rifting proceeds to breakup: Seismicity of the Northern Ethiopian Rift, *J. Geophys. Res.*, *111*, B05314, doi:10.1029/2005JB003748.
Keir, D., I. D. Bastow, K. A. Whaler, E. Daly, D. G. Cornwell, and S. Hautot (2009), Lower crustal earthquakes near the Ethiopian Rift induced by magmatic processes, *Geochem. Geophys. Geosyst.*, *10*, Q0AB02, doi:10.1029/2009GC002382.

Keir, D., C. Pagli, I. D. Bastow, and A. Ayele (2011a), The magma-assisted removal of Arabia in Afar: Evidence from dike injection in the Ethiopian Rift captured using InSAR and seismicity, *Tectonics*, *30*, TC2008, doi:10.1029/2010TC002785.
Keir, D., M. Belachew, C. J. Ebinger, J.-M. Kendall, J. O. S. Hammond, G. W. Stuart, A. Ayele, and J. V. Rowland (2011b), Mapping the evolving strain field during continental breakup from crustal anisotropy in the Afar Depression, *Nat. Commun.*, *2*, 285, doi:10.1038/ncomms1287.
Keir, D., I. D. Bastow, C. Pagli, and E. Chambers (2013), The development of extension and magmatism in the Red Sea Rift of Afar, *Tectonophysics*, *607*, 98–114, doi:10.1016/j.tecto.2012.10.015.
Kendall, J.-M., G. W. Stuart, C. J. Ebinger, I. D. Bastow, and D. Keir (2005), Magma assisted rifting in Ethiopia, *Nature*, *433*, 146–148.
Kendall, J.-M., S. Pilidou, D. Keir, I. Bastow, G. W. Stuart, and A. Ayele (2006), Mantle upwellings, melt migration and the rifting of Africa: Insights from seismic anisotropy, *Geol. Soc. London Spec. Publ.*, *259*, 55–72.
Keranen, K., S. L. Klemperer, R. Gloaguen, and the EAGLE Working Group (2004), Three-dimensional seismic imaging of a protoridge axis in the Main Ethiopian Rift, *Geology*, *32*, 949–952.
Keranen, K., S. L. Klemperer, J. Julia, J. F. Lawrence, and A. A. Nyblade (2009), Low lower crustal velocity across Ethiopia: Is the Main Ethiopian Rift a narrow rift in a hot craton, *Geochem. Geophys. Geosyst.*, *10*, Q0AB01, doi:10.1029/2008GC002293.
Kim, S., A. A. Nyblade, J. Rhie, C. E. Baag, and T. S. Kang (2012), Crustal S-wave velocity structure of the Main Ethiopian Rift from ambient noise tomography, *Geophys. J. Int.*, *191*, 865–878, doi:10.1111/j.1365-246X.2012.05664.x.
Kiyosugi, K., C. B. Connor, P. H. Wetmore, B. P. Ferwerda, A. M. Germa, L. J. Connor, and A. R. Hintz (2012), Relationship between dike and volcanic conduit distribution in a highly eroded monogenetic volcanic field: San Rafael, Utah, USA, *Geology*, *40*, 695–698, doi:10.1130/G33074.1.
Kogan, L., S. Fisseha, R. Bendick, R. Reilinger, S. McClusky, R. King, and T. Solomon (2012), Lithospheric strength and strain localisation in continental extension from observations of the East African Rift, *J. Geophys. Res.*, *117*, B03402, doi:10.1029/2011JB008516.
Le Turdu, C., et al. (1999), The Ziway-Shala lake basin system, Main Ethiopian Rift: Influence of volcanism, tectonics, and climatic forcing on basin formation and sedimentation, *Palaeogeogr. Palaeoclimatol. Palaeoecol.*, *150*, 135–177.
Leroy, S., E. d'Acremont, C. Tiberi, C. Basuyau, J. Autin, F. Lucazeau, and H. Sloan (2010), Recent off-axis volcanism in the eastern Gulf of Aden: Implications for plume-ridge interaction, *Earth Planet. Sci. Lett.*, *293*, 140–153.
Li, C., R. D. van der Hilst, R. Engdahl, and S. Burdick (2008), A new global model for P wave speed variations in Earth's mantle, *Geochem. Geophys. Geosyst.*, *9*, Q05018, doi:10.1029/2007GC001806.
Lizarralde, D., et al. (2007), Variations in styles of rifting in the Gulf of California, *Nature*, *448*, 466–469, doi:10.1038/nature06035.
Maccaferri, F., E. Rivalta, D. Keir, and V. Acocella (2013), Off-rift volcanism in rift zones determined by crustal unloading, *Nat. Geosci.*, *7*, 297–300, doi:10.1038/ngeo2110.
Mackenzie, G. D., H. Thybo, and P. K. H. Maguire (2005), Crustal velocity structure across the Main Ethiopian Rift: Results from two-dimensional wide-angle seismic modelling, *Geophys. J. Int.*, *162*, 994–1006.
Magde, L. S., and D. W. Sparks (1997), Three-dimensional mantle upwelling, melt generation, and melt migration beneath segment slow spreading ridges, *J. Geophys. Res.*, *102*, 20,571–20,583, doi:10.1029/97JB01278.
Maguire, P. K. H., et al. (2006), Crustal structure of the northern Main Ethiopian Rift from the EAGLE controlled source survey: A snapshot of incipient lithospheric break-up, *Geol. Soc. London Spec. Publ.*, *259*, 269–291.
Mazzarini, F., T. Rooney, and I. Isola (2013a), The intimate relationship between strain and magmatism: A numerical treatment of clustered monogenetic fields in the Main Ethiopian Rift, *Tectonics*, *32*, 49–64, doi:10.1029/2012TC003146.
Mazzarini, F., D. Keir, and I. Isola (2013b), Spatial relationship between earthquakes and volcanic vents in the central-northern Main Ethiopian Rift, *J. Volcanol. Geotherm. Res.*, *262*, 123–133, doi:10.1016/j.jvolgeores.2013.05.007.
Mohr, P. A. (1967), Major volcano-tectonic lineament in the Ethiopian rift system, *Nature*, *213*, 664–665, doi:10.1038/213664a0.
Pagli, C., H. Wang, T. J. Wright, E. Calais, and E. Lewi (2014), Current plate boundary deformation of the Afar rift from a 3-D velocity field inversion of InSAR and GPS, *J. Geophys. Res. Solid Earth*, *119*, 8562–8575, doi:10.1002/2014JB011391.
Peccerillo, A., M. R. Barberio, G. Yirgu, D. Ayalew, M. Barbieri, and T. W. Wu (2003), Relationships between mafic and peralkaline silicic magmatism in continental rift settings: A petrological, geochemical and isotopic study of the Gedemsa volcano, central Ethiopian rift, *J. Petrol.*, *44*, 2003–2032.
Ritsema, J., A. Deuss, H. van Heijst, and J. Woodhouse (2011), S40RTS: A degree-40 shear-velocity model for the mantle from new Rayleigh wave dispersion, teleseismic traveltime and normal-mode splitting function measurements, *Geophys. J. Int.*, *184*(3), 1223–1236, doi:10.1111/j.1365-246X.2010.04884.x.
Rooney, T. O. (2010), Geochemical evidence of lithospheric thinning in the southern Main Ethiopian Rift, *Lithos*, *117*, 33–48, doi:10.1016/j.lithos.2010.02.002.
Rooney, T. O., T. Furman, I. Bastow, D. Ayalew, and G. Yirgu (2007), Lithospheric modification during crustal extension in the Main Ethiopian Rift, *J. Geophys. Res.*, *112*, B10201, doi:10.1029/2006JB004916.
Rooney, T. O., I. D. Bastow, and D. Keir (2011), Insights into extensional processes during magma assisted rifting: Evidence from aligned scoria cones, *J. Volcanol. Geotherm. Res.*, *201*, 83–96.
Rooney, T. O., C. Herzberg, and I. D. Bastow (2012a), Elevated mantle temperature beneath East Africa, *Geology*, *40*, 27–30, doi:10.1130/G32382.1.
Rooney, T. O., B. B. Hanan, D. W. Graham, T. Furman, J. Blichert-Toft, and J.-G. Schilling (2012b), Upper mantle pollution during Afar plume—Continental rift interaction, *J. Petrol.*, *53*, 365–389.
Rooney, T. O., W. K. Hart, C. M. Hall, D. Ayalew, M. S. Ghiorso, P. Hidalgo, and G. Yirgu (2012c), Peralkaline magma evolution and the tephra record in the Ethiopian Rift, *Contrib. Mineral. Petrol.*, *164*, 407–426.
Rooney, T. O., P. Mohr, L. Dosso, and C. Hall (2013), Geochemical evidence of mantle reservoir evolution during progressive rifting along the western Afar margin, *Geochim. Cosmochim. Acta*, *102*, 65–88.
Rooney, T. O., I. D. Bastow, D. Keir, F. Mazzarini, E. Movesian, E. B. Grosfils, J. R. Zimbelman, M. S. Ramsay, D. Ayalew, and G. Yirgu (2014a), The protracted development of focused magmatic intrusion during continental rifting, *Tectonics*, *33*, 875–897, doi:10.1002/2013TC003514.
Rooney, T. O., W. R. Nelson, L. Dosso, T. Furman, and B. Hanan (2014b), The role of continental lithosphere metasomes in the production of HIMU-like magmatism on the northeast African and Arabian Plates, *Geology*, *42*, 419–422.
Schaeffer, A., and S. Lebedev (2013), Global shear speed structure of the upper mantle and transition zone, *Geophys. J. Int.*, *194*(1), 417–449.
Schilling, J. G., R. H. Kingsley, B. B. Hanan, and B. L. McCully (1992), Nd-Sr-Pb isotopic variations along the Gulf of Aden: Evidence for Afar mantle plume continental lithosphere interaction, *J. Geophys. Res.*, *97*, 10,927–10,966, doi:10.1029/92JB00415.
Shillington, D. J., C. L. Scott, T. A. Minshull, R. A. Edwards, P. J. Brown, and N. White (2009), Abrupt transition from magma-starved to magma-rich rifting in the eastern Black Sea, *Geology*, *37*, 7–10, doi:10.1130/G25302A.1.
Sleep, N. H. (2008), Channelling at the base of the lithosphere during the lateral flow of plume material beneath flow line hot spots, *Geochem. Geophys. Geosyst.*, *9*, Q08005, doi:10.1029/2008GC002090.

Stamps, S., E. Calais, E. Saria, C. Hartnady, J.-M. Nocquet, C. J. Ebinger, and R. M. Fernandes (2008), Kinematic model for the East African Rift, *Geophys. Res. Lett.*, *35*, L05304, doi:10.1029/2007GL032781.

Tesfaye, S., D. J. Harding, and T. M. Kusky (2003), Early continental breakup boundary and migration of the Afar triple junction, Ethiopia, *Geol. Soc. Am. Bull.*, *115*, 1053–1067, doi:10.1130/B25149.1.

Tibaldi, A. (1995), Morphology of pyroclastic cones and tectonics, *J. Geophys. Res.*, *100*, 24,521–24,535, doi:10.1029/95JB02250.

Trua, T., C. Deniel, and R. Mazzuoli (1999), Crustal control in the genesis of Plio-Quaternary bimodal magmatism of the Main Ethiopian Rift (MER): Geochemical and isotopic (Sr, Nd, Pb) evidence, *Chem. Geol.*, *155*, 201–231.

Ukstins, I. A., P. R. Renne, E. Wolfenden, J. Baker, D. Ayalew, and M. Menzies (2002), Matching conjugate volcanic rifted margins: Ar-40/Ar-39 chrono-stratigraphy of pre- and syn-rift bimodal flood volcanism in Ethiopia and Yemen, *Earth Planet. Sci. Lett.*, *198*, 289–306, doi:10.1016/S0012-821X(02)00525-3.

van Wijk, J. W. (2005), Role of weak zone orientation in continental lithosphere extension, *Geophys. Res. Lett.*, *32*, L02303, doi:10.1029/2004GL022192.

van Wijk, J. W., and D. K. Blackman (2007), Development of en echelon magmatic segments along oblique spreading ridges, *Geology*, *35*, 599–602.

Wang, Y., D. W. Forsyth, and B. Savage (2009), Convective upwelling in the mantle beneath the Gulf of California, *Nature*, *462*, 499–503.

White, R., and D. McKenzie (1989), Magmatism at rift zones: The generation of volcanic continental margins and flood basalts, *J. Geophys. Res.*, *94*, 7685–7729, doi:10.1029/JB094iB06p07685.

White, R. S., L. K. Smith, A. W. Roberts, P. A. F. Christie, N. J. Kusznir, and the rest of the iSIMM Team (2008), Lower-crustal intrusion on the North Atlantic continental margin, *Nature*, *452*, 460–464, doi:10.1038/nature06687.

WoldeGabriel, G., J. L. Aronson, and R. C. Walter (1990), Geology, geochronology, and rift basin development in the central sector of the Main Ethiopia Rift, *Geol. Soc. Am. Bull.*, *102*, 439–458.

Wolfenden, E., C. Ebinger, G. Yirgu, A. Deino, and D. Ayelu (2004), Evolution of the northern Main Ethiopian Rift: Birth of a triple junction, *Earth Planet. Sci. Lett.*, *244*, 213–228.

Wolfenden, E., C. Ebinger, G. Yirgu, P. R. Renne, and S. P. Kelley (2005), Evolution of a volcanic rifted margin: Southern Red Sea, Ethiopia, *Geol. Soc. Am. Bull.*, *117*, 846–864, doi:10.1130/B25516.1.